

# Distribution of $^{36}\text{Cl}$ in the Yoro River Basin, Central Japan, and Its Relation to the Residence Time of the Regional Groundwater Flow System

著者別名	戸崎 裕貴, 田瀬 則雄, 笹 公和
journal or publication title	Water
volume	3
number	1
page range	64-78
year	2011-01
権利	(C) 2011 by the authors; licensee MDPI
URL	<a href="http://hdl.handle.net/2241/107814">http://hdl.handle.net/2241/107814</a>

doi: 10.3390/w3010064

Article

## Distribution of $^{36}\text{Cl}$ in the Yoro River Basin, Central Japan, and Its Relation to the Residence Time of the Regional Groundwater Flow System

Yuki Tosaki <sup>1,\*</sup>, Norio Tase <sup>2</sup>, Akihiko Kondoh <sup>3</sup>, Kimikazu Sasa <sup>4</sup>, Tsutomu Takahashi <sup>4</sup> and Yasuo Nagashima <sup>4</sup>

<sup>1</sup> Crustal Fluid Research Group, Geological Survey of Japan, National Institute of Advanced Industrial Science and Technology (AIST), Tsukuba Central 7, 1-1-1 Higashi, Tsukuba, Ibaraki 305-8567, Japan

<sup>2</sup> Sustainable Environmental Studies, Graduate School of Life and Environmental Sciences, University of Tsukuba, 1-1-1 Tennodai, Tsukuba, Ibaraki 305-8572, Japan;  
E-Mail: tase@geoenv.tsukuba.ac.jp

<sup>3</sup> Center for Environmental Remote Sensing (CEReS), Chiba University, 1-33 Yayoi, Inage, Chiba 263-8522, Japan; E-Mail: kondoh@faculty.chiba-u.jp

<sup>4</sup> Tandem Accelerator Complex, Research Facility Center for Science and Technology, University of Tsukuba, 1-1-1 Tennodai, Tsukuba, Ibaraki 305-8577, Japan;  
E-Mails: ksasa@tac.tsukuba.ac.jp (K.S.); takahasi@tac.tsukuba.ac.jp (T.T.); nagashima@tac.tsukuba.ac.jp (Y.N.)

\* Author to whom correspondence should be addressed; E-Mail: yuki.tosaki@aist.go.jp;  
Tel.: +81-29-861-3087; Fax: +81-29-861-3087.

Received: 10 December 2010; in revised form: 22 December 2010 / Accepted: 24 December 2010 /  
Published: 6 January 2011

---

**Abstract:** This study investigates the potential of  $^{36}\text{Cl}$  in tracing young groundwater with residence times of up to ~50 years. Groundwater samples were obtained from 16 irrigation wells in paddy fields located within an upland–lowland system in the Yoro River basin, Central Japan. The  $^{36}\text{Cl}/\text{Cl}$  ratios were in the range of 17 to  $362 \times 10^{-15}$ . Among the samples with higher  $\text{Cl}^-$  concentrations (>10 mg/L), two samples showed high nitrate concentrations as well (>30 mg/L). Except for these samples, the distribution of  $^{36}\text{Cl}$  in groundwater was essentially consistent with previous tritium concentration data measured in 1982 and 1994, considering the time that has elapsed since these earlier measurements

were performed.  $^{36}\text{Cl}/\text{Cl}$  values were less than  $30 \times 10^{-15}$  in lowland areas, with higher values in and around upland areas. The results indicate longer residence times in the regional groundwater flow system (>50 years) than those estimated in previous studies, especially in the area west of the Yoro River. The results demonstrate the ability of  $^{36}\text{Cl}$  to trace young groundwater flow, particularly because high values of bomb-derived  $^{36}\text{Cl}/\text{Cl}$  are easily discriminated from pre-bomb water with low  $^{36}\text{Cl}/\text{Cl}$  values. Because of its very long half-life ( $3.01 \times 10^5$  years),  $^{36}\text{Cl}$  remains even after tritium is no longer available.

**Keywords:** groundwater flow system; residence time; environmental tracer;  $^{36}\text{Cl}$ ; accelerator mass spectrometry (AMS)

---

## 1. Introduction

In recent decades, groundwater has been extensively used for drinking, agricultural, and industrial purposes; consequently, its depletion has become a serious problem in many areas worldwide, such as the North China Plain [1] and the High Plains of the United States [2]. Because the mean residence time of groundwater reservoir is typically long (~1,400 years [3]), groundwater is highly vulnerable to excess use and contamination; in the case of groundwater depletion or contamination, aquifers require a long time for recovery and purification.

Therefore, an understanding of groundwater flow systems and groundwater residence time is an important component of the sustainable management of water resources. The use of environmental tracers (see Figure 1) is one of the most effective approaches in visualizing the movement of groundwater (e.g., [4,5]). Tritium ( $^3\text{H}$ ) has been commonly used in hydrologic studies during the last several decades. However, due to its short half-life (12.32 years [6]), tritium concentration has largely returned to the pre-bomb (natural) background level.

Bomb-produced  $^{36}\text{Cl}$  is an alternative to tritium [7,8], as it is a long-lived radioisotope of chlorine with a half-life of  $3.01 \times 10^5$  years, decaying to  $^{36}\text{Ar}$  by  $\beta$  emission (98.10%) and to  $^{36}\text{S}$  by electron capture (1.90%) [9]. Natural  $^{36}\text{Cl}$  in the hydrologic cycle originates mainly from cosmic ray spallation of  $^{40}\text{Ar}$  in the stratosphere. The global mean production rate of  $^{36}\text{Cl}$  in the atmosphere is estimated to be  $21.4 \text{ atoms m}^{-2} \text{ s}^{-1}$  [10], which is much lower than that of lighter long-lived radionuclides produced from nitrogen and oxygen (e.g.,  $^{10}\text{Be}$  and  $^{14}\text{C}$ ).

After production,  $^{36}\text{Cl}$  leaves the stratosphere and enters the troposphere within about two years [11]. The  $^{36}\text{Cl}$  produced in the atmosphere is mixed with marine-derived stable chlorine (from sea spray), and falls rapidly as wet or dry deposition onto the earth's surface. The mean residence time in the troposphere is expected to be in the order of weeks, according to estimates of residence times for atmospheric aerosols [12-14].

In addition to natural production, significant amounts of  $^{36}\text{Cl}$  were produced by thermonuclear testing on small islands or barges (mainly at Bikini and Eniwetok atolls in 1954, 1956, and 1958 [15]). Neutrons released from the testing activated  $^{35}\text{Cl}$  in seawater. Some of this bomb-produced  $^{36}\text{Cl}$  reached the stratosphere and spread over the globe. The fallout of bomb-produced  $^{36}\text{Cl}$  preserved in ice cores (e.g., [11]) shows a peak in the late 1950s. Due to the relatively low abundance of  $^{35}\text{Cl}$  in the

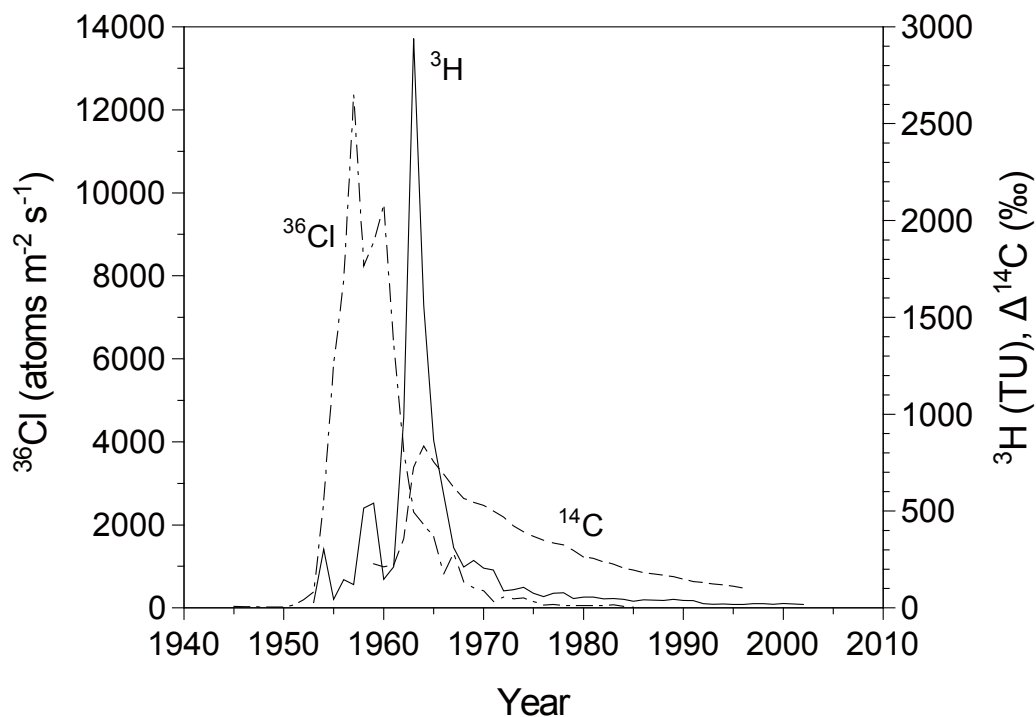
atmosphere, atmospheric tests have a negligible contribution to the production of  $^{36}\text{Cl}$ , resulting in the time lag between the  $^3\text{H}$  and  $^{36}\text{Cl}$  peaks ( $\sim 7$  years; see Figure 1)

Chlorine has a high electron affinity and exists predominantly as the chloride anion ( $\text{Cl}^-$ ) in the environment [16]. It generally does not participate in redox reactions and biochemical processes, and is not absorbed onto mineral surfaces except under conditions of low pH [17,18]. Hence, it moves with water in the natural hydrological cycle without significant chemical interaction. Its simple geochemistry and conservative behavior make chloride an ideal tracer in hydrology [19]. In addition, it is straightforward to collect samples for analyses of chloride and chlorine isotopes.

The advantage of bomb-produced  $^{36}\text{Cl}$  as a hydrological tracer is derived from the fact that the peak is well defined, and that the long half-life of  $^{36}\text{Cl}$  makes decay attenuation negligible on the time scale of several decades to centuries (e.g., [20,21]). In previous studies, the  $^{36}\text{Cl}$  bomb pulse has been used to trace water movement in the unsaturated zone, especially in arid and semi-arid regions (e.g., [22–24]); however, few studies have applied this method to tracing young groundwater [25,26]. In combination with  $^3\text{H}$ , bomb-produced  $^{36}\text{Cl}$  has been used to estimate the rate of groundwater recharge in a fractured rock aquifer [25] and to deduce the flow velocity and dispersivity in a sandy aquifer [26].

The aim of the present study is to investigate the potential of  $^{36}\text{Cl}$  in tracing a regional groundwater flow system with a time scale of  $\sim 50$  years. This paper reports on the observed  $^{36}\text{Cl}$  distribution in groundwater beneath an upland–lowland topographic system, and compares the results with existing tritium data. The distribution of  $^{36}\text{Cl}$  observed in the present study has implications for the tracer properties of  $^{36}\text{Cl}$ , including the bomb-derived component.

**Figure 1.** Atmospheric concentrations or fallout rates of bomb-derived environmental tracers (after [27]):  $^{36}\text{Cl}$  fallout rates at the Dye-3 site, Greenland [11];  $^3\text{H}$  concentration in precipitation at Ottawa, Canada [28]; and atmospheric  $\delta^{14}\text{C}$  record at Vermont, Austria (1959–1983); and Schauinsland, Germany (1984–1996) [29].

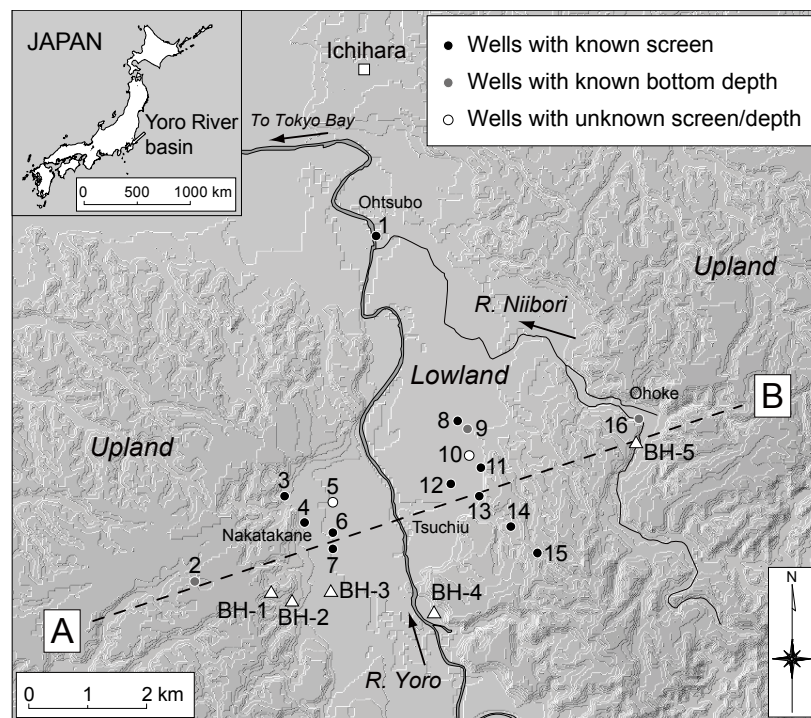


## 2. Study Site and Methods

### 2.1. Topography, Geology, and Climate

The study area is located in the lower part of the Yoro River basin, northern Boso Peninsula, Central Japan (Figure 2). The Yoro River runs northward through the central part of the area into Tokyo Bay. The area is characterized by fluvial terraces and alluvial lowlands along the river, and surrounding Pleistocene uplands and hills. The uplands and hills are part of the Shimosa Upland and Kazusa Hills, respectively. The upland surface slopes northwestward, at elevations ranging from ~100 m in the south to ~40 m along Tokyo Bay in the north.

**Figure 2.** Locations of sampled irrigation wells in the Yoro River basin. Open triangles indicate selected borehole locations from Kondoh (1985) [30] and Chiba Prefectural Research Institute for Environmental Pollution (1974) [31].



The following geological summary of the study area is based on Tokuhashi and Endo (1984) [32]. The area is dominated by (in ascending stratigraphic order) middle Pleistocene upper Kazusa Group sediments, middle–upper Pleistocene Shimosa Group sediments, upper Pleistocene terrace deposits with Kanto Loam, Holocene terrace deposits, and alluvial deposits. The Kazusa and Shimosa groups strike northeast–southwest, dipping gently northwest at 0.4–6.0°. The alluvium is distributed mainly in the lowlands along the Yoro River, with lesser amounts in dissected valleys in the hills and uplands.

The Kazusa Group occurs extensively throughout the Kazusa Hills in the middle to northern part of the Boso Peninsula. Of the 12 formations in this group, only the upper formations (*i.e.*, the Kokumoto, Kakinokidai, Chonan, Kasamori, and Kongochi formations, in ascending stratigraphic order) are exposed in the study area. The Kazusa Group is composed mainly of alternating deep-water sand and mudstone, with lesser shallow-water sandy mudstone, sand, and cross-bedded gravelly sands.

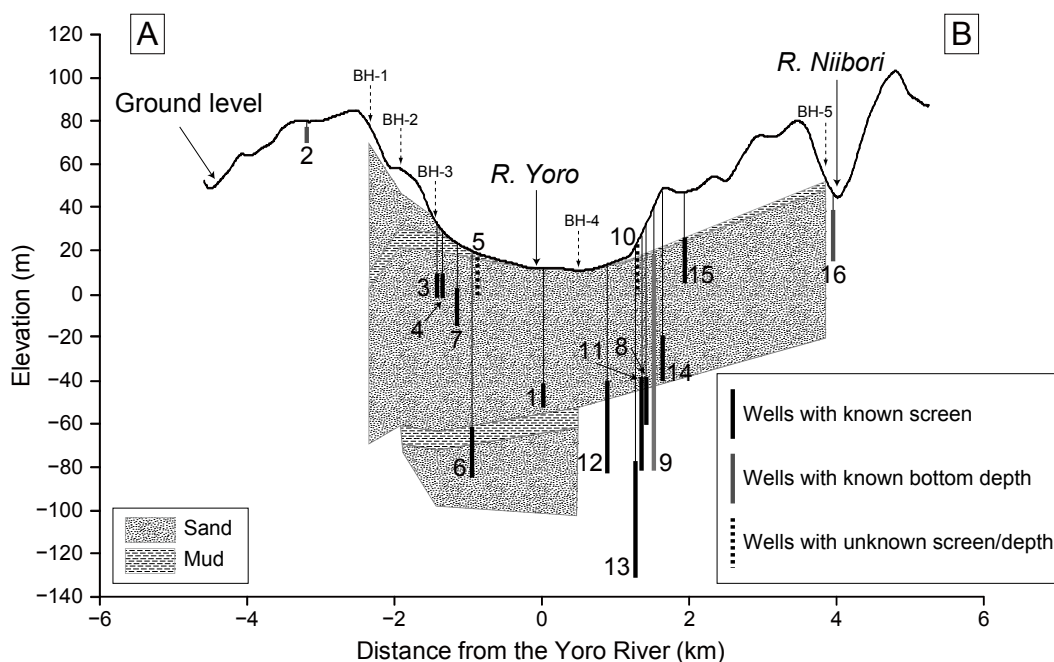
The Shimosa Group, which overlies the Kazusa Group, is widely exposed in the Shimosa Uplands, in the northern part of Boso Peninsula. This group consists of seven formations (*i.e.*, the Jizodo, Yabu, Kamiizumi, Kiyokawa, Yokota, Kioroshi, and Anesaki formations, in ascending stratigraphic order), with a maximum total thickness of over 250 m. The uppermost Anesaki Formation consists of fresh-water sediments. Other formations in the group are characterized by sedimentary cycles that start from fresh- or brackish-water muds and end with shallow-marine sands.

The study area is located in a humid temperate climate, with an annual mean temperature of  $\sim 15$  °C and average annual precipitation ranging from 1,294 mm at Chiba on the northwestern side of the study area, near the coast along Tokyo Bay, to 1,590 mm at Ushiku in the southern hilly area (average values for 1971–2000 [33]). The estimated annual evapotranspiration rate is  $\sim 700$  mm at Chiba [30].

## 2.2. Hydrogeology

In this area, the Kasamori Formation, which is dominated by muddy sandstone, probably acts as the hydraulic basement for the groundwater in the overlying Shimosa Group sediments. Mainly in the upland regions, groundwater is used extensively for irrigation and drinking water. The main aquifers supplying the groundwater located within the Jizodo and Yabu formations, which is composed by alternating sand and mud [30] (Figure 3). The depth to the water table is generally small, e.g., 3–5 m at Nakatakane area (near wells 3, 4, and 7),  $\sim 3$  m at Ohtsubo area (near well 1), and  $\sim 3$  m at Ohoke area (near well 16) [31] (see Figure 2 for the locations). Thus, the shape of the water table is expected to reflect the surface topography. Aquifer tests showed relatively high hydraulic conductivities ( $10^{-3}$ – $10^{-2}$  cm/s) in this area [30].

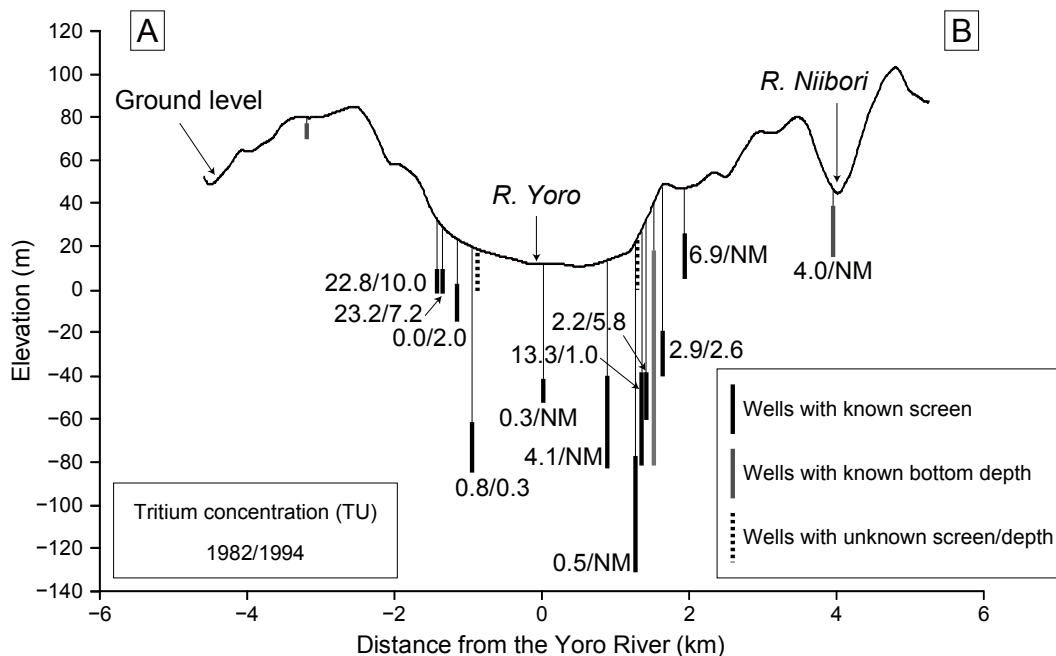
**Figure 3.** Cross-section showing the geology and the distribution of well screens projected onto the line A–B in Figure 2. The screen intervals or bottom depths of the wells are given in Table 1. Geological data is from Kondoh (1985) [30] and Chiba Prefectural Research Institute for Environmental Pollution (1974) [31] (see Figure 2 for the borehole locations).



Kondoh (1985) [30] performed a three-dimensional numerical simulation of regional groundwater flow in this area. The results revealed the importance of topographic controls on the groundwater flow, as well as the minor contribution of the northwestward dip of the geological structure. These findings were confirmed by the distribution of tritium concentrations in groundwater within the basin [30]: High tritium concentrations occur in the upland region, and low concentrations in the lowland region, along the Yoro River (Figure 4). This distribution indicates the occurrence of relatively young groundwater ages in the upland region, and older ages in the lowland area. It also shows that recharge occurs mainly in upland areas and that groundwater essentially flows into the lowland area, eventually discharging into the Yoro River. Because groundwater samples in the lowland area showed very low tritium concentrations at that time (1982), the regional groundwater flow system from the upland to lowland region appears to have a residence time greater than 30 years (recharged before 1953; see Figure 1).

In 1994, Miyazawa (1995) [34] revisited the regional groundwater flow system in the Yoro River basin by measuring tritium concentrations in groundwater samples obtained from some of the locations sampled previously by Kondoh (1985) [30]. Even though 12 years had passed since the first study, groundwater in the lowland area still contained low tritium concentrations (Figure 4). This observation clearly indicates the presence of pre-bomb groundwater recharged before 1953 (age > 40 years).

**Figure 4.** Tritium concentrations measured in 1982 [30] and 1994 [34]. Left and right values for each well are tritium data measured in 1982 and 1994, respectively. Wells without values indicate that tritium data are unavailable. NM: not measured.



### 2.3. Methodology

Sites for groundwater sampling for  $^{36}\text{Cl}$  measurements were mainly irrigation wells for which tritium data are available [30,34]. Sampling was performed during the irrigation period for paddy

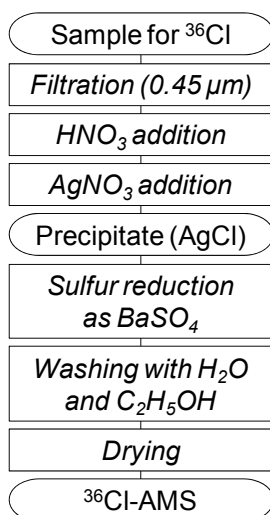


fields in the summer of 2004 (24 July and 13 August). Sixteen groundwater samples were collected from pumped irrigation wells located within the basin, ranging from lowland to upland areas (Figure 2).

The samples were analyzed for dissolved inorganic ions, silica, stable isotopes of oxygen and hydrogen, and  $^{36}\text{Cl}$ , at the University of Tsukuba, Japan. Prior to chemical analyses, the samples were passed through 0.20  $\mu\text{m}$  filters (25HP020AN, Advantec, Tokyo, Japan). Concentrations of major dissolved cations ( $\text{Na}^+$ ,  $\text{K}^+$ ,  $\text{Mg}^{2+}$ , and  $\text{Ca}^{2+}$ ) and silica ( $\text{SiO}_2$ ) were measured with an ICP–AES (inductively coupled plasma–atomic emission spectroscopy) system (ICAP-757, Nippon Jarrell-Ash, Kyoto, Japan). Bicarbonate ( $\text{HCO}_3^-$ ) concentrations were determined by titration with dilute  $\text{H}_2\text{SO}_4$  solution. Concentrations of major anions ( $\text{Cl}^-$ ,  $\text{NO}_3^-$ , and  $\text{SO}_4^{2-}$ ) were measured by ion chromatography (QIC Analyzer, Dionex, Sunnyvale, CA, U.S.). Stable isotopic ratios of oxygen and hydrogen ( $\delta^{18}\text{O}$  and  $\delta\text{D}$ ) were determined with a mass spectrometer (MAT252, Thermo Finnigan, Bremen, Germany). The analytical errors were 0.1‰ and 1‰ for  $\delta^{18}\text{O}$  and  $\delta\text{D}$ , respectively.

Figure 5 summarizes the preparation procedure used in this study. All samples for measurements of  $^{36}\text{Cl}$  by AMS ( $^{36}\text{Cl}$ -AMS) were passed through 0.45  $\mu\text{m}$  filters (JHWP04700, Millipore). The samples were then processed according to the preparation scheme shown in Figure 5. Water samples containing  $\sim 1$  mg of Cl were acidified with 1 mL of 13 M of  $\text{HNO}_3$ . Chloride was then precipitated as silver chloride ( $\text{AgCl}$ ) by adding excess  $\text{AgNO}_3$ , and was separated by centrifugation. The  $\text{AgCl}$  precipitate was dissolved once in 3 M of  $\text{NH}_4\text{OH}$ , and saturated  $\text{Ba}(\text{NO}_3)_2$  solution was added to the solution. The solution was allowed to stand overnight in an oven at  $\sim 60$  °C, to effectively precipitate  $\text{SO}_4^{2-}$  as  $\text{BaSO}_4$ . This precipitate was removed by filtration with a 0.20  $\mu\text{m}$  membrane filter (25HP020AN, Advantec), and the filtrate was acidified by the addition of 13 M of  $\text{HNO}_3$  to precipitate  $\text{AgCl}$  again.

**Figure 5.** Summary of the sample preparation scheme for  $^{36}\text{Cl}$ -AMS.



Because the isobar  $^{36}\text{S}$  (natural abundance, 0.02% [9]) strongly interferes with  $^{36}\text{Cl}$  measurements by accelerator mass spectrometry (AMS), the chemical reduction of sulfur is of major importance in preparing  $\text{AgCl}$  samples. The removal of sulfur (in the form of  $\text{SO}_4^{2-}$ ) can be achieved by the precipitation of  $\text{BaSO}_4$  (e.g., [35]), by differential elution from an anion exchange resin [36], or by absorption onto a cation exchange resin (in the form of  $\text{BaSO}_4$ ) [37]. The main part of sample preparation, including sulfur reduction, was performed in an air-conditioned room to prevent



additional sulfur contamination and was performed under dark conditions to avoid the photolytic decomposition of AgCl.

The sample was purified by repeated precipitation of AgCl with HNO<sub>3</sub> and dissolution in NH<sub>4</sub>OH. To further exclude remaining impurities, the AgCl precipitate was washed with Milli-Q ultrapure water twice and with 99.5% C<sub>2</sub>H<sub>5</sub>OH twice using ultrasonic vibration. The overall chemical yield of chlorine was typically about 80%. For subsequent <sup>36</sup>Cl-AMS, a benzene solution saturated with fullerene (C<sub>60</sub>) was added to each sample (~20 μL per 1 mg of AgCl) and the sample was dried in an oven at 120 °C for more than 24 hours. Finally, the sample was pressed into the target holder for <sup>36</sup>Cl-AMS.

<sup>36</sup>Cl/Cl ratios were measured using the AMS system at the Tandem Accelerator Complex, Research Facility Center for Science and Technology, University of Tsukuba [38], along with diluted NIST <sup>36</sup>Cl standards (<sup>36</sup>Cl/Cl = 1.60 × 10<sup>-12</sup> [39]). The electric current of <sup>35</sup>Cl<sup>-</sup> was measured by a Faraday cup located immediately after the ion source, whereas <sup>36</sup>Cl ions were counted at the final detector, being distinguished from <sup>36</sup>S. The <sup>36</sup>Cl/<sup>35</sup>Cl<sup>-</sup> ratio (counts/μC) derived from the measurements was normalized to that obtained for the standard sample. The obtained <sup>36</sup>Cl/Cl ratio of the sample was subjected to a background correction using the measured ratio of a chemical blank prepared from a sample of Himalayan halite. The overall precision of the system was better than 2%, and the background level of <sup>36</sup>Cl/Cl was ~1 × 10<sup>-15</sup> [38]. The calculated <sup>36</sup>Cl/Cl ratio of the sample includes the statistical error derived from the uncertainties (1σ) calculated for the sample, the standard, and the blank.

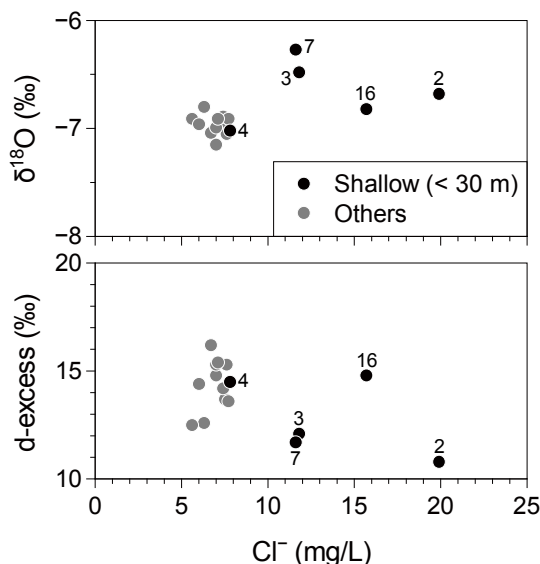
### 3. Results and Discussions

Table 1 lists the stable isotopic compositions and <sup>36</sup>Cl data for the analyzed samples, along with existing data for tritium [30,34]. Major dissolved ions and SiO<sub>2</sub> concentrations are given in Table 2. Samples 2, 3, 7, and 16, show much higher Cl<sup>-</sup> concentrations than the other samples (Table 2). Samples 2 and 16, which were taken from shallow wells (<30 m; Table 1) located far from the Yoro River, have high NO<sub>3</sub><sup>-</sup> concentrations (>30 mg/L), indicating the influence of agricultural fertilizers. This trend of nitrate contamination is confirmed by a Piper diagram (Figure 6). These two samples (Samples 2 and 16) may contain anthropogenic chloride derived from fertilizer, which would lower their original <sup>36</sup>Cl/Cl values to some extent; consequently, these samples were excluded from the discussion on the distribution of <sup>36</sup>Cl/Cl values. Although the <sup>36</sup>Cl/Cl values obtained for Sample 2 are not considered in the interpretations presented below, the low SiO<sub>2</sub> concentration obtained for this sample (Table 2) suggests a young groundwater age.

The stable isotopic compositions showed a relatively small variation mostly in the range of -7.1‰ to -6.8‰ and -43‰ to -40‰ for δ<sup>18</sup>O and δD, respectively, although the bottom depth (or screen depth) of the wells varies from ~10 m to ~100 m. This range of variation is almost consistent with the results of a δ<sup>18</sup>O-δD mapping study of surface waters and shallow groundwaters in Japan [40]. The small variation may indicate that the investigated aquifers of the study area are recharged at almost similar elevation, probably in upland areas. Shallow wells tend to show slightly higher stable isotopic ratios, while deeper wells have lower δ<sup>18</sup>O and δD values (Table 1; Figure 6). This may suggest an influence of a local recharge from the surface, which can possess higher δ<sup>18</sup>O and δD values. Among the samples with high Cl<sup>-</sup> concentrations, Samples 2, 3, and 7 show relatively low d-excess values

(Table 1; Figure 6), as defined by  $d = 8\delta^{18}\text{O} - \delta\text{D}$ , that may indicate the influence of evaporation. Because evaporation does not affect  $^{36}\text{Cl}/\text{Cl}$  values, Samples 3 and 7 are considered in the following discussion.

**Figure 6.**  $\delta^{18}\text{O}$  and d-excess values for groundwater plotted against the  $\text{Cl}^-$  concentrations.



**Table 1.**  $^{36}\text{Cl}$  and isotopic data for groundwater samples from the Yoro River basin.

Sample No.	Depth (m)	$^{36}\text{Cl}/\text{Cl}$ ( $10^{-15}$ )	$^{36}\text{Cl}$ ( $10^6$ atoms/L)	$^3\text{H}_a$ (TU)	$^3\text{H}_b$ (TU)	$\delta^{18}\text{O}$ (‰)	$\delta\text{D}$ (‰)	d-excess (‰)
1	48–60	$25 \pm 3$	$2.7 \pm 0.3$	$0.3 \pm 0.3$	NM	-6.8	-42	12.6
2	10	$61 \pm 5$	$20.6 \pm 1.8$	NM	NM	-6.7	-43	10.8
3	14–27	$140 \pm 9$	$27.9 \pm 1.8$	$22.8 \pm 0.5$	$10.0 \pm 1.3$	-6.5	-40	12.1
4	24–27	$150 \pm 9$	$19.9 \pm 1.2$	$23.2 \pm 0.5$	$7.2 \pm 1.2$	-7.0	-42	14.5
5	NK	$29 \pm 20$	$2.8 \pm 1.9$	NM	NM	-6.9	-43	12.5
6	80–105	$17 \pm 3$	$1.8 \pm 0.3$	$0.8 \pm 0.3$	$0.3 \pm 0.5$	-7.0	-41	14.4
7	18–32	$117 \pm 10$	$23.1 \pm 2.0$	$0.0 \pm 0.4$	$2.0 \pm 1.1$	-6.3	-38	11.7
8	54–78	$258 \pm 11$	$33.2 \pm 1.5$	$5.8 \pm 0.8$	$5.8 \pm 0.8$	-7.1	-41	15.3
9	100	$161 \pm 14$	$21.2 \pm 1.9$	NM	NM	-6.9	-42	13.6
10	NK	$65 \pm 13$	$7.8 \pm 1.6$	NM	NM	-7.0	-41	14.8
11	56–100	$128 \pm 8$	$15.4 \pm 1.0$	$13.3 \pm 0.5$	$1.0 \pm 0.6$	-6.9	-40	15.4
12	56–100	$216 \pm 13$	$27.5 \pm 1.7$	$4.1 \pm 0.3$	NM	-6.9	-42	13.7
13	95–150	$362 \pm 20$	$43.2 \pm 2.4$	$0.5 \pm 0.5$	$5.5 \pm 1.0$	-7.1	-42	15.3
14	50–72	$225 \pm 15$	$28.2 \pm 1.9$	$2.9 \pm 0.6$	$2.6 \pm 0.9$	-6.9	-41	14.2
15	32–54	$345 \pm 17$	$39.4 \pm 2.0$	$6.9 \pm 0.6$	NM	-7.0	-40	16.2
16	25	$243 \pm 18$	$65.1 \pm 4.8$	$4.0 \pm 0.4$	$11.8 \pm 1.4$	-6.8	-40	14.8

NK: not known.

NM: not measured.

$^3\text{H}_a$ : tritium concentration measured in 1982 [30].

$^3\text{H}_b$ : tritium concentration measured in 1994 [34].

**Table 2.** Dissolved major ions and silica concentrations in groundwater from the Yoro River basin.

Sample No.	Na <sup>+</sup> (mg/L)	K <sup>+</sup> (mg/L)	Mg <sup>2+</sup> (mg/L)	Ca <sup>2+</sup> (mg/L)	Cl <sup>-</sup> (mg/L)	NO <sub>3</sub> <sup>-</sup> (mg/L)	SO <sub>4</sub> <sup>2-</sup> (mg/L)	HCO <sub>3</sub> <sup>-</sup> (mg/L)	SiO <sub>2</sub> (mg/L)
1	7.7	7.3	7.9	30.6	6.3	0.2	4.0	143.4	45.6
2	8.9	5.2	11.6	15.9	19.9	93.3	0.1	6.1	18.8
3	9.5	7.1	9.2	48.2	11.8	0.8	29.3	163.5	55.6
4	10.4	10.7	8.7	28.3	7.8	0.3	7.1	142.7	43.1
5	9.3	8.1	7.2	25.1	5.6	0.2	8.1	118.3	55.5
6	19.4	7.7	7.5	24.3	6.0	0.2	8.2	151.3	57.3
7	10.6	5.9	14.4	42.1	11.6	0.2	2.7	280.6	47.6
8	9.4	7.5	11.2	42.6	7.6	0.2	25.5	160.4	57.9
9	9.5	7.8	10.0	36.3	7.7	0.2	16.2	150.7	62.0
10	8.0	6.4	7.8	25.4	7.0	0.3	10.6	111.0	60.3
11	8.8	7.0	9.5	32.2	7.1	2.2	15.1	133.6	63.1
12	7.6	7.2	6.4	25.3	7.5	0.2	13.3	100.0	54.9
13	8.4	5.6	9.0	22.6	7.0	0.2	15.8	103.7	60.5
14	8.6	7.3	7.5	39.2	7.4	0.2	14.6	145.8	52.5
15	7.2	6.2	7.1	13.6	6.7	3.4	10.4	68.9	65.6
16	11.3	7.5	16.8	35.4	15.7	32.0	10.3	143.4	61.2

**Figure 7.** Chemical compositions of groundwater shown in a Piper diagram.

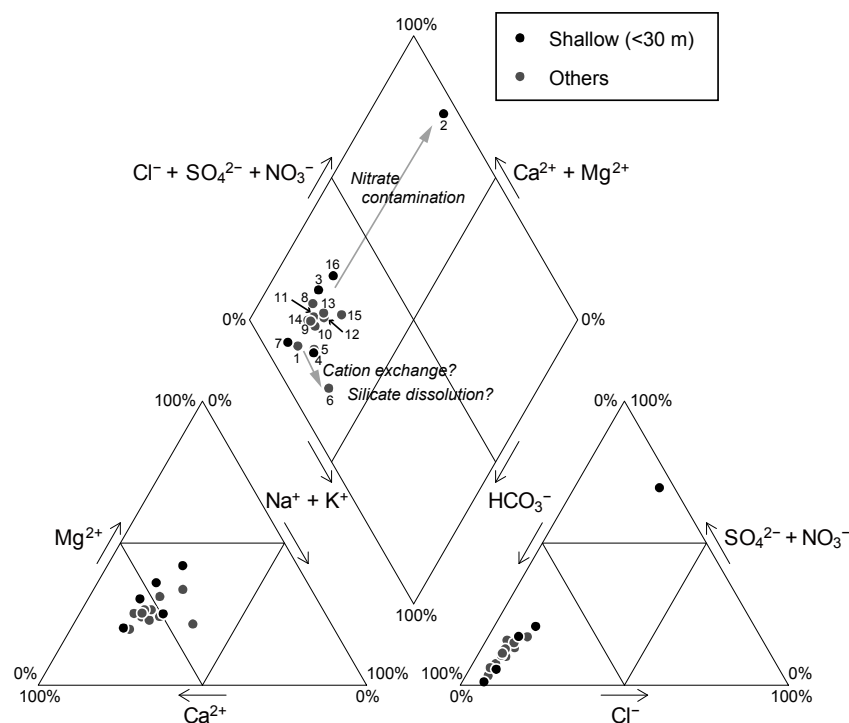
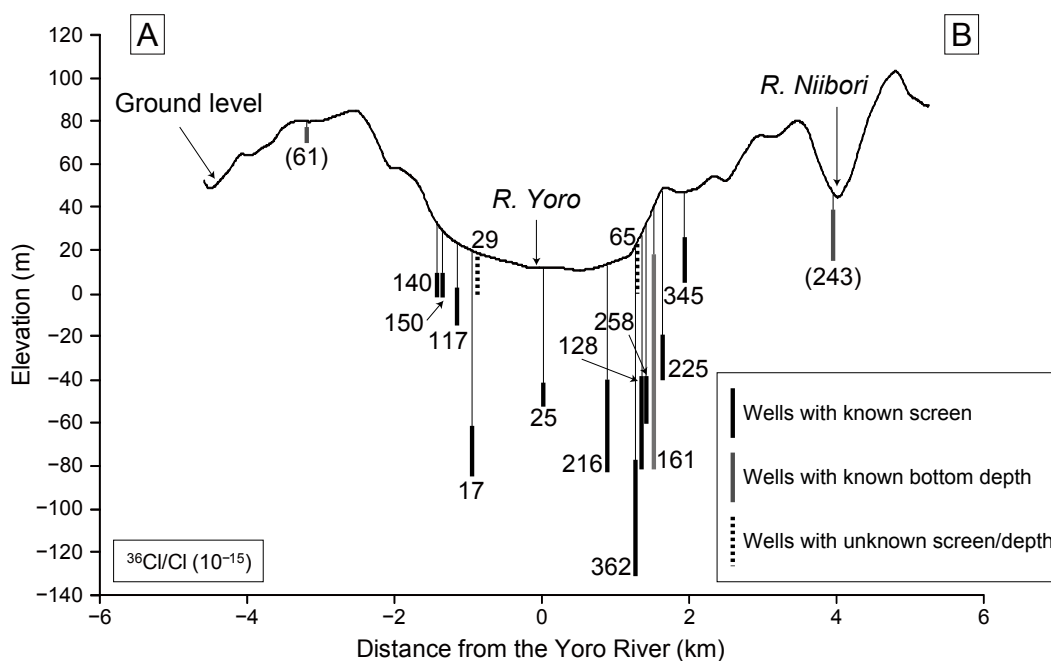


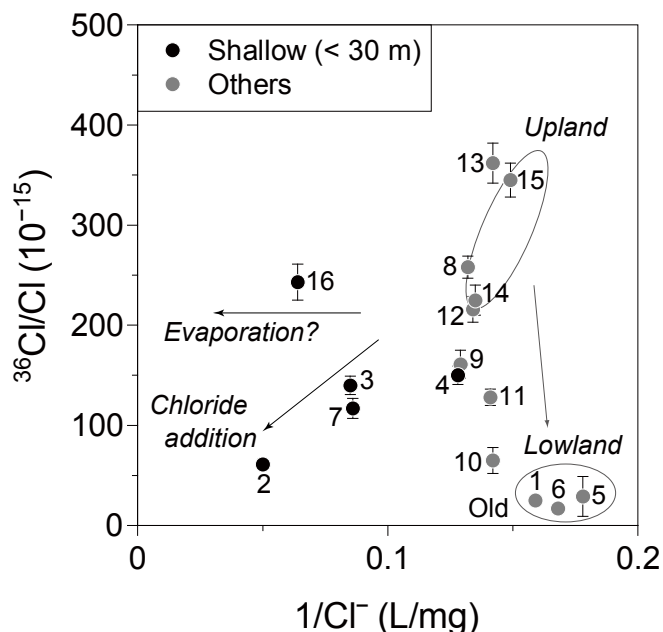
Figure 8 shows the distribution of <sup>36</sup>Cl/Cl values projected onto the line A–B in Figure 2. Although Sample 1 is located relatively far from the projection line, it was also included because it represents groundwater in the discharge area. The overall distribution shows low <sup>36</sup>Cl/Cl values in the lowland area along the river, and higher values toward upland areas, except for nitrate-contaminated samples.

The observed distribution is basically consistent with the groundwater flow system traced by tritium in 1982 and 1994 (Figure 4), which showed relatively high concentrations in upland areas and low concentrations in lowland areas. One difference in this regard is that relatively high  $^{36}\text{Cl}/\text{Cl}$  values are found near the upland area on the eastern side of the Yoro River. This result is expected if we consider the time that has passed since tritium concentrations were measured, as the groundwater could have flowed further toward the lowland area during this time.

**Figure 8.** Cross-sectional distribution of  $^{36}\text{Cl}/\text{Cl}$  values in the Yoro River basin. Parentheses indicate samples with high  $\text{NO}_3^-$  concentrations.



To further examine the nature of hydrological processes operating in the basin, Figure 9 shows  $^{36}\text{Cl}/\text{Cl}$  values plotted against the reciprocal of  $\text{Cl}^-$  concentrations. Samples obtained from shallow wells (<30 m) show higher  $\text{Cl}^-$  concentrations than do the other samples, which again suggests the influence of non-meteoric chloride and/or evaporation. Among the remaining samples (*i.e.*, samples from deeper wells, including two samples from unknown depths), two samples from the upland area (Samples 14 and 15) have high  $^{36}\text{Cl}/\text{Cl}$  values (Figure 8). The  $^{36}\text{Cl}/\text{Cl}$  values has a roughly decreasing trend northwestward from well 15 to well 10, except for wells 8 and 9 (Figures 2 and 8). Because these wells are located slightly north of the Tsuchiu area (Figure 2), they are possibly on a different flow line from the other samples. Conversely, three representative samples of the lowland area (Samples 1, 5, and 6), show markedly low  $^{36}\text{Cl}/\text{Cl}$  values ( $<30 \times 10^{-15}$ ). This difference demonstrates that pre-bomb (*i.e.*, ages > 50 years) groundwater remains in the lowland area, suggesting residence times in excess of 50 years for the regional groundwater flow system, which is longer than that estimated previously (up to 40 years) [30,34]. Because most of the other samples, except for the lowland samples, show elevated  $^{36}\text{Cl}/\text{Cl}$  values, their ages are likely to be in the range of 25–50 years (see Figure 1).

**Figure 9.**  $^{36}\text{Cl}/\text{Cl}$  values for groundwater plotted against the reciprocal of  $\text{Cl}^-$  concentrations.

The  $\text{Na}/\text{Cl}$  molar ratios of the three lowland samples (Samples 1, 5, and 6) tend to have higher values (1.9, 2.5, and 5.0, respectively) than those of the other samples (0.7–2.1), as calculated from Table 2. This result may reflect a cation exchange reaction between  $\text{Ca}^{2+}$  in groundwater and  $\text{Na}^+$  in the matrix materials of the aquifer, or silicate dissolution (see Figure 7). Because the content of TDS (total dissolved solids) in Sample 6 shows no significant increase compared with that in other samples, the high  $\text{Na}/\text{Cl}$  value may have been derived mainly from a cation exchange reaction.

Considering the slightly lower  $\text{Cl}^-$  concentrations in lowland samples compared with upland samples (Figure 9), it is possible that human activity (anthropogenic chloride derived from the application of agricultural fertilizer) has had an increasing influence on recharging groundwater (mainly in the upland area). However, this would not lead to a significant contribution on the observed  $^{36}\text{Cl}/\text{Cl}$  ratios, as indicated by the slight increase in chloride concentrations (~20%). The remarkably high  $\text{Na}/\text{Cl}$  value for Sample 6 suggests it has a relatively old age, which in turn supports the interpretations based on the distribution of  $^{36}\text{Cl}$  throughout the basin.

#### 4. Conclusions

We investigated the potential of  $^{36}\text{Cl}$  in tracing young groundwater with residence times of up to ~50 years. The  $^{36}\text{Cl}/\text{Cl}$  values of groundwater within the Yoro River basin ranged from 17 to  $362 \times 10^{-15}$ . The cross-sectional distribution of  $^{36}\text{Cl}$  in groundwater is essentially consistent with previous tritium data measured in 1982 and 1994, given the time that has elapsed since these earlier measurements were performed. Low  $^{36}\text{Cl}/\text{Cl}$  values, of the order of  $10^{-14}$ , were found only in lowland areas, whereas the upland area was dominated by higher values. This finding suggests longer residence times in the regional groundwater flow system than those estimated previously, especially in the area west of the Yoro River.

The present results show the ability of  $^{36}\text{Cl}$  to trace young groundwater flow, because relatively high values of bomb-derived  $^{36}\text{Cl}/\text{Cl}$  are easily discriminated from the low values of pre-bomb water.

The long half-life of bomb-produced  $^{36}\text{Cl}$  ( $3.01 \times 10^5$  years) enables its use as an environmental tracer over a long period even after tritium is no longer available for use. Therefore,  $^{36}\text{Cl}$  is an important alternative to tritium as a groundwater tracer for young groundwater.

### Acknowledgements

Yuki Tosaki thanks the members of the AMS Group at the University of Tsukuba for their contribution to measurements of  $^{36}\text{Cl}$ . Yuki Tosaki also thanks the staff at the Chiba Prefectural Agriculture and Forestry Promotion Center, Japan, for providing the well location data. The authors wish to thank all the technical staff at UTTAC (University of Tsukuba Tandem Accelerator Complex) for their support during operation of the accelerator. This paper was financially supported in part by a Grant-in-Aid for Scientific Research (B) (No. 21310004) from the Japan Society for the Promotion of Science (JSPS) and a research grant (No. 22343) from the Kurita Water and Environment Foundation (KWEF), Japan.

### References

1. Foster, S.; Garduno, H.; Evans, R.; Olson, D.; Yuan T.; Weizhen Z.; Zaisheng H. Quaternary aquifer of the North China Plain—assessing and achieving groundwater resources sustainability. *Hydrogeol. J.* **2004**, *12*, 81-93.
2. Sophocleous, M. Review: Groundwater management practices, challenges, and innovations in the High Plains aquifer, USA—lessons and recommended actions. *Hydrogeol. J.* **2010**, *18*, 559-575.
3. Oki, T. The hydrologic cycles and global circulation. In *Encyclopedia of Hydrological Sciences*; Anderson, M.G., McDonnell, J.J., Eds.; John Wiley & Sons, Ltd.: Chichester, UK, 2005; Volume 1, pp. 13-22.
4. Egboka, B.C.E.; Cherry, J.A.; Farvolden, R.N.; Frind, E.O. Migration of contaminants in groundwater at a landfill: A case study 3. Tritium as an indicator of dispersion and recharge. *J. Hydrol.* **1983**, *63*, 51-80.
5. Robertson, W.D.; Cherry, J.A. Tritium as an indicator of recharge and dispersion in a groundwater system in central Ontario. *Water Resour. Res.* **1989**, *25*, 1097-1109.
6. Lucas, L.L.; Unterweger, M.P. Comprehensive review and critical evaluation of the half-life of tritium. *J. Res. NIST* **2000**, *105*, 541-549.
7. Bentley, H.W.; Phillips, F.M.; Davis, S.N.; Gifford, S.; Elmore, D.; Tubbs, L.E.; Gove, H.E. Thermonuclear  $^{36}\text{Cl}$  pulse in natural water. *Nature* **1982**, *300*, 737-740.
8. Tosaki, Y.; Tase, N.; Massmann, G.; Nagashima, Y.; Seki, R.; Takahashi, T.; Sasa, K.; Sueki, K.; Matsuhira, T.; Miura, T.; Bessho, K.; Matsumura, H.; He, M. Application of  $^{36}\text{Cl}$  as a dating tool for modern groundwater. *Nucl. Instrum. Methods Phys. Res. B* **2007**, *259*, 479-485.
9. Firestone, R.B.; Shirley, V.S. *Table of Isotopes*, 8th ed.; John Wiley & Sons, Ltd.: New York, NY, USA, 1996; Volume 1.
10. Masarik, J.; Beer, J. An updated simulation of particle fluxes and cosmogenic nuclide production in the Earth's atmosphere. *J. Geophys. Res.* **2009**, *114*, D11103.
11. Synal, H.-A.; Beer, J.; Bonani, G.; Suter, M.; Wölfli, W. Atmospheric transport of bomb-produced  $^{36}\text{Cl}$ . *Nucl. Instrum. Methods Phys. Res. B* **1990**, *52*, 483-488.

12. Turekian, K.K.; Nozaki, Y.; Benninger, L.K. Geochemistry of atmospheric radon and radon products. *Ann. Rev. Earth Planet. Sci.* **1977**, *5*, 227-255.
13. Bleichrodt, J.F. Mean tropospheric residence time of cosmic-ray-produced beryllium 7 at north temperate latitudes. *J. Geophys. Res.* **1978**, *83*, 3058-3062.
14. Raisbeck, G.M.; Yiou, F.; Fruneau, M.; Loiseaux, J.M.; Lieuvin, M.; Ravel, J.C. Cosmogenic  $^{10}\text{Be}/^7\text{Be}$  as a probe of atmospheric transport processes. *Geophys. Res. Lett.* **1981**, *8*, 1015-1018.
15. Zerle, L.; Faestermann, T.; Knie, K.; Korschinek, G.; Nolte, E.; Beer, J.; Schotterer, U. The  $^{41}\text{Ca}$  bomb pulse and atmospheric transport of radionuclide. *J. Geophys. Res.* **1997**, *102*, 19517-19527.
16. Bentley, H.W.; Phillips, F.M.; Davis, S.N. Chlorine-36 in the terrestrial environment. In *Handbook of Environmental Isotope Geochemistry*; Fritz, P., Fontes, J.-Ch., Eds.; Elsevier: Amsterdam, The Netherlands, 1986; Volume 2, pp. 427-480.
17. Feth, J.H.F. *Chloride in Natural Continental Water: A review*; U.S. Department of the Interior, U.S. Geological Survey: Reston, VA, USA and Washington, DC, USA, 1981.
18. Hem, J.D. *Study and Interpretation of the Chemical Characteristics of Natural Water*, 3rd ed.; U.S. Geological Survey: Reston, VA, USA, 1985; p. 263.
19. Herczeg, A.L.; Edmunds, W.M. Inorganic ions as tracers. In *Environmental Tracers in Subsurface Hydrology*; Cook, P.G., Herczeg, A.L., Eds.; Kluwer: Boston, MA, USA, 2000; pp. 31-77.
20. Fabryka-Martin, J.; Davis, S.N.; Elmore, D. Applications of  $^{129}\text{I}$  and  $^{36}\text{Cl}$  in hydrology. *Nucl. Instrum. Methods Phys. Res. B* **1987**, *29*, 361-371.
21. Fontes, J.-Ch.; Andrews, J.N. Accelerator mass spectrometry in hydrology. *Nucl. Instrum. Methods Phys. Res. B* **1994**, *92*, 367-375.
22. Phillips, F.M.; Mattick, J.L.; Duval, T.A.; Elmore, D.; Kubik, P.W. Chlorine 36 and tritium from nuclear weapons fallout as tracers for long-term and vapor movement in desert soils. *Water Resour. Res.* **1988**, *24*, 1877-1891.
23. Scanlon, B.R. Evaluation of liquid and vapor flow in desert soils based on chlorine 36 and tritium tracers and nonisothermal flow simulations. *Water Resour. Res.* **1992**, *28*, 285-297.
24. Cook, P.G.; Jolly, I.D.; Leaney, F.W.; Walker, G.R. Unsaturated zone tritium and chlorine 36 profiles from southern Australia: Their use as tracers of soil water movement. *Water Resour. Res.* **1994**, *30*, 1709-1719.
25. Cook, P.G.; Robinson, N.I. Estimating groundwater recharge in fractured rock from environmental  $^3\text{H}$  and  $^{36}\text{Cl}$ , Clare Valley, South Australia. *Water Resour. Res.* **2002**, *38*, 1136.
26. Balderer, W.; Synal, H.-A.; Deak, J. Application of the chlorine-36 method for the delineation of groundwater infiltration of large river systems: Example of the Danube River in western Hungary (Szigetköz area). *Environ. Geol.* **2004**, *46*, 755-762.
27. Cook, P.G.; Böhlke, J.K. Determining timescales for groundwater flow and solute transport. In *Environmental Tracers in Subsurface Hydrology*; Cook, P.G., Herczeg, A.L., Eds.; Kluwer: Boston, MA, USA, 2000; pp. 1-30.
28. International Atomic Energy Agency and World Meteorological Organization. *Global Network of Isotopes in Precipitation: The GNIP Database*. Available online: <http://www.iaea.org/water> (accessed on 4 October 2007).



29. Carbon Dioxide Information Analysis Center, Oak Ridge National Laboratory, United States Department of Energy. *Trends Online: A Compendium of Data on Global Change*. Available online: <http://cdiac.esd.ornl.gov/trends/trends.htm> (accessed on 4 October 2007).
30. Kondoh, A. *Study on the Groundwater Flow System by Environmental Tritium in Ichihara Region, Chiba Prefecture*; Environmental Research Center, University of Tsukuba: Ibaraki, Japan, 1985; Volume 6, p. 59.
31. *Groundwater Movement and Landsubsidence Phenomena in the Groundwater Basin (in Japanese)*; Project Research Report, No. 2; Chiba Prefectural Research Institute for Environmental Pollution: Funabashi, Japan, 1974.
32. Tokuhashi, S.; Endo, H. *Geology of the Anesaki District, Quadrangle Series, Scale 1:50,000 (in Japanese with English abstract)*; Geological Survey of Japan: Tsukuba, Japan, 1984; p. 136.
33. Japan Meteorological Agency. *Weather Observation: Climate Statistics (in Japanese)*. Available online: <http://www.data.jma.go.jp/obd/stats/etrn/index.php> (accessed on 3 May 2010).
34. Miyazawa, N. *Groundwater Flow System in Ichihara Area Cleared by Environmental Tritium (in Japanese with English Abstract)*; Bachelor's Thesis; College of Natural Sciences, University of Tsukuba: Tsukuba, Japan, 1995.
35. Conard, N.; Elmore, D.; Kubik, P.; Gave, H.; Tubbs, L.; Chrnyk, B.; Wahlen M. The chemical preparation of AgCl for measuring  $^{36}\text{Cl}$  in polar ice with accelerator mass spectrometry. *Radiocarbon* **1986**, *28*, 556-560.
36. Vogt, S.; Herpers, U. Radiochemical separation techniques for the determination of long-lived radionuclides in meteorites by means of accelerator-mass-spectrometry. *Fresenius' Z. Anal. Chem.* **1988**, *331*, 186-188.
37. Jiang, S.; Lin, Y.; Zhang, H. Improvement of the sample preparation method for AMS measurement of  $^{36}\text{Cl}$  in natural environment. *Nucl. Instrum. Methods Phys. Res. B* **2004**, *223-224*, 318-322.
38. Sasa, K.; Takahashi, T.; Tosaki, Y.; Matsushi, Y.; Sueki, K.; Tamari, M.; Amano, T.; Oki, T.; Mihara, S.; Yamato, Y.; Nagashima, Y.; Bessho, K.; Kinoshita, N.; Matsumura, H. Status and research programs of the multinuclide accelerator mass spectrometry system at the University of Tsukuba. *Nucl. Instrum. Methods Phys. Res. B* **2010**, *268*, 871-875.
39. Sharma, P.; Kubik, P.W.; Fehn, U.; Gove, H.E.; Nishiizumi, K.; Elmore, D. Development of  $^{36}\text{Cl}$  standards for AMS. *Nucl. Instrum. Methods Phys. Res. B* **1990**, *52*, 410-415.
40. Mizota, C.; Kusakabe, M. Spatial distribution of  $\delta^{18}\text{O}$ - $\delta\text{D}$  values of surface and shallow groundwaters from Japan, south Korea and east China. *Geochem. J.* **1994**, *28*, 387-410.